

## Photoionization of magnesium from the excited $3snd\ ^1D$ states to the doubly excited $3pnl\ ^1F$ autoionization states

T. N. Chang and X. Tang

*Department of Physics, University of Southern California, Los Angeles, California 90089-0484*

(Received 22 February 1988)

We present the result of a theoretical estimation of the photoionization cross sections for transitions from the excited  $3snd\ ^1D$  states of Mg to the doubly excited  $3pnl\ ^1F$  autoionization states above the first ionization threshold. In particular, we examine in detail the effect of the multielectron interactions both in the initial and the final states of the transition. The calculated excitation energy and the width for the  $3pnl\ ^1F$  autoionization series are reported. The experimental implications are also discussed.

### I. INTRODUCTION

At an energy immediately above the first ionization threshold, the spectra of the alkaline-earth atoms are dominated by the strongly energy-dependent doubly excited autoionization states. Most of the early experimental works are limited to transitions initiated from the ground state of the atom.<sup>1-5</sup> In general, the doubly excited autoionization states of all allowed symmetries corresponding to total spin  $S$ , total orbital angular momentum  $L$ , and total angular momentum  $J$  can be generated in an *electron-impact energy-loss* experiment.<sup>1</sup> In spite of the presence of states of all possible symmetries in the energy-loss spectra, the substantial overlap of these states and the dominance of few strong transitions often make it difficult to characterize in detail those autoionization states corresponding to the weak transitions. On the other hand, the autoionization states reached by the dipole transition from the ground state (e.g.,  $^1P$  states) can often be identified with little ambiguity in an *optical experiment*<sup>2-5</sup> as the transitions to the final states corresponding to other symmetries are either weakened or forbidden due to the dipole selection rule.

The autoionization structures observed in the photoionization from the ground state often exhibit an asymmetric profile due to the configuration interaction between the quasibound doubly excited state and the background open channel.<sup>6</sup> For states of relatively large width, the photoionization cross section from the ground state is relatively modest with values ranging from a few Mb ( $10^{-18}$  cm<sup>2</sup>) to less than 100 Mb at or near the resonance energy. When the background cross section due to the direct transition from the initial state to the ionization background accounts for a large portion of the maximum cross section, the resulting strongly asymmetric autoionization structure could make the precise determination of its position and width difficult.

To study in detail the autoionization states other than those corresponding to the  $^1P$  symmetry, an early attempt was made in a photoelectron experiment<sup>7</sup> with a high-resolution laser to photoionize the Mg atom from the initial  $3s3p\ ^1P$  state to the final  $3p^2\ ^1S$  autoionization state.

More recently, in a multistep multicolor photoionization experiment, by detecting the Mg ions, Bonanno *et al.*<sup>8</sup> confirmed the excitation energy and the width of the Mg  $3p^2\ ^1S$  autoionization state measured in the earlier photoelectron experiment. The availability of high-resolution intense uv laser, together with the fact that the photoionization cross sections for strong transitions from *excited states* to the autoionization states are often of the order of several hundred Mb (i.e., about one to two orders of magnitude higher than the typical cross sections for the optical transitions from the ground state), have opened up the possibility of *systematic high resolution characterization* of the doubly excited autoionization structures of all possible symmetries. For *strong* transitions from the *excited states*, the background photoionization cross section is generally much smaller than the maximum cross section at the resonance energy and the autoionization structure is mostly symmetric.<sup>7-9</sup> As a result, the resonance energy and the autoionization width can be determined experimentally with a higher degree of accuracy.

A detailed theoretical study of the photoionization from the excited states of the alkaline-earth atom parallel to this new experimental possibility would undoubtedly lead to a more precise physical interpretation of the multielectron interaction in a many-electron atomic system, as the initial and final states of transition are both highly correlated. In this paper, we will examine the photoionization of Mg from the excited  $3snd\ ^1D$  states to the  $3pmd\ ^1F$  autoionization series above the first ionization threshold. The  $3snd\ ^1D$  series are chosen as the possible initial states of the photoionization for the reason that the oscillator strengths  $f$  for the  $3s3p\ ^1P$  to  $3snd\ ^1D$  transitions remain significant as  $n$  increases (e.g.,  $f=0.246$ , 0.108, 0.118 and 0.085 for  $n=3-6$  states<sup>10</sup>), thus in a multistep process, even for a state with a medium  $n$  can still be generated with sufficient population for the subsequent photoionization measurement. In addition to the quantitative estimation of the photoionization cross sections near the dominating autoionization structures, we will also study in detail the effect of the initial-state configuration interaction on the redistribution of the photoionization cross sections due to the  $3pn(\geq 3)p$

configuration series. The final-state interactions between the doubly excited quasibound components and the ionization background are also examined.

## II. CALCULATIONAL PROCEDURE

Similar to a recent photoionization calculation for transition from the Mg  $3s3p^1P$  state to the  $3p^2^1S$  autoionization state,<sup>9</sup> a simple superposition of configuration wave-function (SCW) procedure<sup>11,12</sup> is employed to construct the initial  $3snd^1D$  multiconfiguration-state wave function  $\Phi_{3snd}(^1D)$ , i.e.,

$$\Phi_{3snd}(^1D) = \sum_{n_1 l_1 n_2 l_2} C_{3snd}(n_1 l_1 n_2 l_2) \psi_{n_1 l_1 n_2 l_2}(^1D), \quad (1)$$

where  $\psi_{n_1 l_1 n_2 l_2}$  is the  $^1D$  single-configuration wave function corresponding to a two-electron configuration  $n_1 l_1 n_2 l_2$  outside the  $^1S$  frozen core of  $N-2$  electrons. The set of expansion coefficients  $C_{3snd}$  corresponding to the  $3snd^1D$  state diagonalizes the Hamiltonian matrix which includes the nonrelativistic  $N$ -electron Hamiltonian, the core dipole polarization potential,<sup>9</sup> and the dielectronic interaction.<sup>13</sup> The state wave function  $\Psi_E$  representing the doubly excited  $3pnd^1F$  autoionization state is given by<sup>6,9,14</sup>

$$\Psi_E = \left[ \sum + \int \right] a_{n(\epsilon)f}(E) \psi_{3sn(\epsilon)f} + \sum_{\nu\mu} b_{\nu\mu}(E) \Phi_{\nu\mu}, \quad (2)$$

where the expansion coefficients  $a_{n(\epsilon)f}$  and  $b_{\nu\mu}$  are functions of energy  $E$ . The first expansion term over the single-configuration wave function  $\psi_{3sn(\epsilon)f}$  represents the combined contribution from the bound ( $nf$ ) and the continuum ( $\epsilon f$ ) parts of the  $^1F$  background open channel to the state wave function  $\Psi_E$ . The multiconfiguration bound components of the state wave function are represented by  $\Phi_{\nu\mu}$  in the second term of Eq. (2). The bound part of the background open channel, i.e.,  $\psi_{3snf}$ , included in the first term of Eq. (2), are excluded from the SCW calculation of  $\Phi_{\nu\mu}$  which represents a multiconfiguration function dominated by the  $n_\nu l_\nu n_\mu l_\mu$  configuration. The expansion coefficients  $a_{n(\epsilon)f}$  and  $b_{\nu\mu}$  are determined by the procedure similar to the original one developed by Fano<sup>6</sup> and outlined elsewhere.<sup>9,14</sup> The photoionization cross sections for the  $3snd^1D$  to  $3pnd^1F$  transition are calculated by the procedure given in Ref. 9. The widths and the excitation energies of the  $3pnl^1F$  autoionization states are determined by the procedure given in Ref. 14.

## III. RESULTS AND DISCUSSION

The calculated photoionization cross sections  $\sigma$  (in  $10^{-16}$  cm<sup>2</sup> or 100 Mb) from the Mg  $3sn(3-6)d^1D$  excited states to the  $3pm(3-4)d^1F$  autoionization states are shown as functions of wavelength (in nanometers) in Fig. 1. The broader structure on the longer-wavelength side corresponds to the  $3p3d^1F$  autoionization state and the narrower one on the shorter-wavelength side corresponds to the  $3p4d^1F$  state. For a strong transition with cross section larger than 100 Mb, the autoionization structure

is generally symmetric, while for the weaker transition with cross section less than 50 Mb, the asymmetric nature of the autoionization structure becomes more prominent. The presence of such a highly symmetric autoionization structure for the strong transitions from the excited states would make the determination of the width and the resonance energy much less ambiguous, as we suggested earlier. Our calculated photoionization cross sections in the dipole length and velocity approximations are in *close agreement* at all energies, as illustrated by the solid (length) and dotted (velocity) curves in the  $3s3d^1D$  to  $3pnd^1F$  spectrum shown in Fig. 1. Similarly, for other spectra included in the present calculation, the length results are slightly higher than the velocity values and only the velocity results are presented in Fig. 1.

To illustrate the effect of the many-electron interaction in the  $^1D$  initial state of the photoionization (e.g., the strong configuration mixing with the  $3pnp$  configuration series), we have also carried out calculations with the  $3pnp$  series *excluded* from the construction of the initial-state multiconfiguration wave function  $\Phi_{3snd}$ . The photoionization spectra of such a calculation for transitions from the  $3s4d^1D$  initial state to the final autoionization structures including  $3p3d$ ,  $3p4d$ ,  $3p5g$ , and  $3p5d^1F$  states are represented by the top curves shown in Fig. 2. The

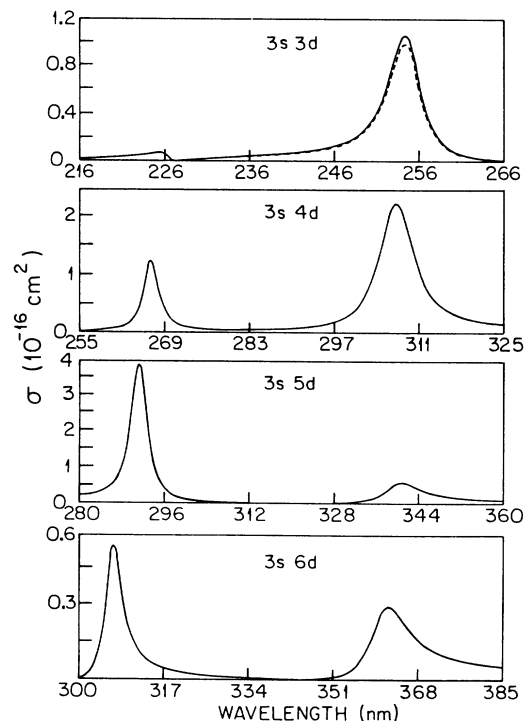


FIG. 1. Calculated photoionization cross sections  $\sigma$  (in  $10^{-16}$  cm<sup>2</sup>) from the excited  $3snd^1D$  states of Mg to the doubly excited  $3p(3-4)d^1F$  autoionization states. The autoionization structure on the longer-wavelength side corresponds to the  $3p3d^1F$  state and the one on the shorter-wavelength side corresponds to the  $3p4d^1F$  state. The solid curve in the photoionization spectrum from  $3s3d^1D$  state represents the dipole-length results, while the dotted curve represents the dipole-velocity results. For all other spectra, only velocity results are given.

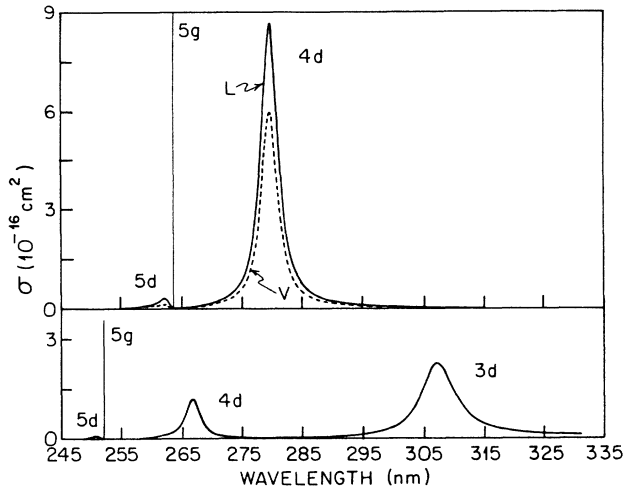


FIG. 2. Photoionization cross sections  $\sigma$  (in  $10^{-16} \text{ cm}^2$ ) from the  $3s4d \ ^1D$  state of Mg to the  $3pnl \ ^1F$  autoionization states calculated *with* (bottom) and *without* (top) the contribution from the  $3pnp$  configuration series in the initial  $3s4d \ ^1D$  state wave functions. Both length ( $L$ ) and velocity ( $V$ ) results are given in the top diagram. Only the velocity results are presented in the bottom diagram as the length and velocity values are in close agreement.

effect of the  $3pnp$  configuration series to the initial state can be measured by the difference between this spectrum and the calculated spectrum *with the  $3pnp$  series included* (i.e., the bottom spectrum in Fig. 2). First, in the absence of the  $3pnp$  series, the cross section to the final  $3p3d \ ^1F$  state is practically zero. Second, the calculated length (solid curve) results are at least 40% higher than the velocity (dotted curve) results. Third, the calculated excitation energies of the autoionization states are shifted substantially from our final results. Fourth, a substantial redistribution of the photoionization cross sections is observed when we include the  $3pnp$  series in the initial-state wave function. This effect is similar to the redistribution of the oscillator strength observed in the bound-bound  $3snd \ ^1D$  to  $3smf \ ^1F$  transitions,<sup>10</sup> which is illustrated in Table I, where the calculated oscillator strengths  $f$  are

listed for the  $3s4d \ ^1D$  to  $3sn(4-7)f \ ^1F$  transitions *with* (first column) and *without* (second column) the contribution from the  $3pnp$  configuration series to the  $3s4d \ ^1D$  state.

We now turn our attention to the effect of the many-electron interaction in the  $^1F$  final state of the transition. Following our recent photoionization study,<sup>9</sup> the dipole transition matrix  $D$  is separated into three contributing terms, i.e.,

$$D = D_1 + D_2 + D_3, \quad (3)$$

where  $D_1$  and  $D_2$  represent the direct transitions from the initial state to the ionization background [i.e.,  $3sn(\epsilon)f$  open channel] and the doubly excited multiconfiguration *bound* components  $\Phi_{\nu\mu}$ , respectively. The contribution from the final-state interaction between the  $3sn(\epsilon)f$  background and the doubly excited bound components  $\Phi_{\nu\mu}$  is given by the third term  $D_3$ . As an example, Fig. 3 illustrates the relative contributions from each of these three terms to the total photoionization cross section  $\sigma$  (in  $10^{-16} \text{ cm}^2$ ) for the  $3s4d \ ^1D$  to  $3pn(3-4)d \ ^1F$  transition in the dipole length calculation. The solid curve  $A$  represents the final result when all three terms are included. The dashed curve  $B$  represents the calculated result with the  $D_1$  term excluded. In general, for strong transitions, the background contribution from the direct transition to the ionization background is small, as shown by the relatively small difference between curves  $A$  and  $B$ . The dotted curve  $C$  represents the calculated results with the  $D_3$  term excluded. The contribution from the  $D_3$  term, which measures the strength of the final-state interaction, is represented by the difference between the dotted curve  $C$  and the solid curve  $A$ . Our calculation has shown that the effect of the final-state interaction is generally stronger in the length calculation than in the velocity calculation (not shown). For the  $3s4d \ ^1D$  to  $3pnd \ ^1F$  transition, the final-state interaction has led to a substantial reduction in cross sections for the  $3s4d-3p3d$  transition on the longer-wavelength side and a factor of 5 or more increase in cross sections for the  $3s4d-3p4d$  transition on the shorter-wavelength side shown in Fig. 3.

TABLE I. The redistribution of the calculated oscillator strengths  $f$  for the  $3s4d \ ^1D$  to  $3snf \ ^1F$  transitions due to the effect from the  $3pnp$  configuration series in the  $3s4d \ ^1D$  state wave function. The first column represents the  $f$  values in the length ( $L$ ) and velocity ( $V$ ) calculations *without* the  $3pnp$  series, and the second column represents the  $f$  values *with* the  $3pnp$  series.  $f$  values are taken from our recent calculation (Ref. 10).

Transition	$f$ (without $3pnp$ series)	$f$ (with $3pnp$ series)
$4d-4f$	0.086 ( $L$ )	0.653 ( $L$ )
	0.087 ( $V$ )	0.654 ( $V$ )
$4d-5f$	1.001 ( $L$ )	0.120 ( $L$ )
	1.005 ( $V$ )	0.120 ( $V$ )
$4d-6f$	0.175 ( $L$ )	0.064 ( $L$ )
	0.172 ( $V$ )	0.063 ( $V$ )
$4d-7f$	0.062 ( $L$ )	0.035 ( $L$ )
	0.061 ( $V$ )	0.035 ( $V$ )

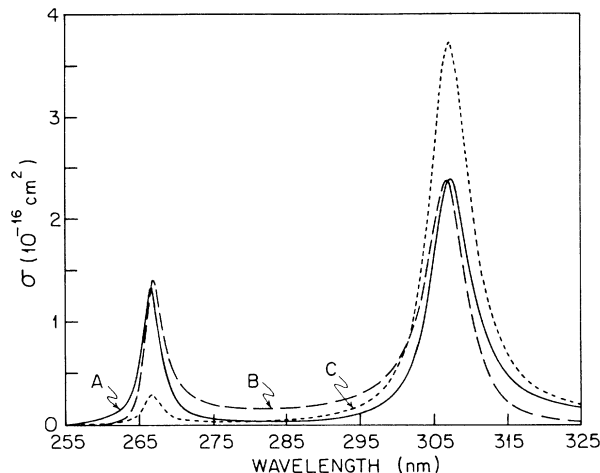


FIG. 3. Calculated photoionization cross sections  $\sigma$  (in  $10^{-16}$   $\text{cm}^2$ ) from the  $3s4d\ ^1D$  state of Mg to the  $3p(3-4)d\ ^1F$  states in the dipole-length approximation. The solid curve *A* represents the final result including contributions from all three terms (i.e.,  $D_1$ - $D_3$ ). The dashed curve *B* represents the results excluding the contribution from the  $D_1$  term. The dotted curve *C* represents the results excluding the contribution from the  $D_3$  term.

Similar to the recent  $3s3p\ ^1P$  to  $3p^2\ ^1S$  calculation,<sup>9,14</sup> all the results presented so far are calculated with the lowest  $^1F$  configuration  $3s4f$  excluded from the first term of Eq. (2). In this combination (denoted as calculation *A*), the short-range interaction due to the  $3s4f$  configuration is included as a part of a total of 16  $\Phi_{3pnl}$  terms which represent the bound components of the  $3pnl\ ^1F$  autoionization series. To further examine the strength of this type of short-range interaction, we have carried out calculations *with* contribution from the  $3s4f$  configuration *included* in the first term of Eq. (2) and in this alternative combination (denoted as calculation *B*), only 15  $\Phi_{3pnl}$  terms are included in the second term. The main difference between these two calculations is that the orbital wave function for the  $4f$  orbit is calculated with a *one-particle Hartree-Fock Hamiltonian*  $h^{\text{HF}}$  [i.e., Eq. (9) of Ref. 11] in *A*, while the *one-particle screening Hamiltonian*  $h_l$  [i.e., Eq. (8) of Ref. 9] is used in *B*. The calculated photoionization cross sections from *A* and *B* are very close to each other except at energies near the resonance energy. Figure 4 shows that the peak cross sections in the velocity approximation for the  $3s4d\ ^1D$  to  $3pnd\ ^1F$  transition from calculation *B* [Fig. 4(b)] are slightly smaller than the values from calculation *A* [Fig. 4(a)]. The difference between the peak cross sections of these two calculations results primarily from the difference in the calculated widths given in Table II as the peak cross section is inversely proportional to the width of the autoionization state.<sup>6,9</sup> The excitation energies from the  $3s3d\ ^1D$  state are generally in close agreement between calculations *A* and *B*, despite the noticeable difference in the calculated widths. We should also note that the excitation energies reported in Table II are

determined with the calculated phase shift  $\Delta$  following the procedure outlined in Ref. 14. For *weak* transition, the *excitation energy* may be *different* from the energy at the peak photoionization cross section due to the asymmetric nature of the autoionization structure. For higher members in the  $3pnl\ ^1F$  autoionization series, the effect due to the different treatment of the short-range interaction between the doubly excited  $3pnl$  configuration series and the  $3s4f$  configuration diminishes as the interaction between the  $3pnl$  configuration and the  $3s4f$  becomes negligible.

In addition, a less elaborate lowest-order estimation of the excitation energies and the widths of the  $3pnl\ ^1F$  autoionization series similar to the one used in the recent study<sup>14</sup> of the Mg  $3s3p\ ^1P$  to  $3p^2\ ^1S$  transition has been carried out by including only the multiconfiguration bound component  $\Phi_{\nu\mu}$  in our calculation. The results are listed in parentheses in Table II. For the lowest  $3p3d\ ^1F$  state, the final-state interaction between the  $3sn(\epsilon)f$  background open channel and the bound components  $\Phi_{\nu\mu}$  of the autoionization state has reduced the difference in excitation energy from approximately  $400\ \text{cm}^{-1}$  to about  $20\ \text{cm}^{-1}$  and at the same time the difference in width from about 40% to 20%. The widths for the narrow  $3png\ ^1F$  states are very sensitive to the numbers of  $\Phi_{\nu\mu}$  included in the fitting procedure<sup>14</sup> with values ranging between  $0.001\ \text{cm}^{-1}$  and  $1\ \text{cm}^{-1}$ .

Based on the close agreement between the result of our recent theoretical calculation and the experimental measurement for the Mg  $3s3p\ ^1P$  to  $3p^2\ ^1S$  transition,<sup>9,14</sup> it

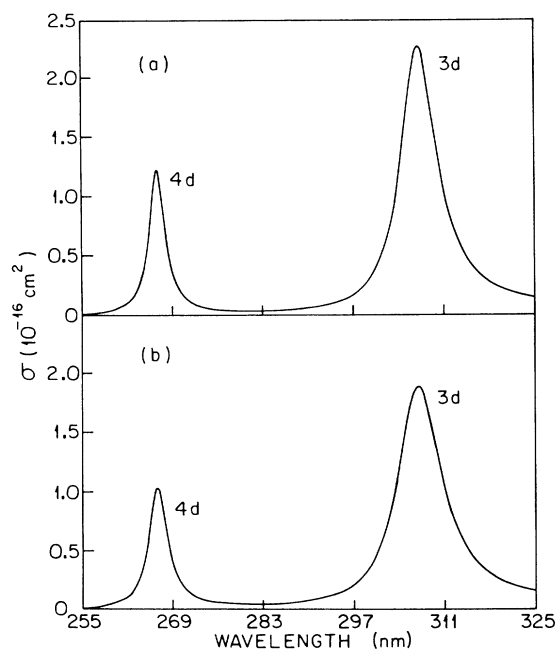


FIG. 4. Calculated photoionization cross sections  $\sigma$  (in  $10^{-16}$   $\text{cm}^2$ ) for transitions from the  $3s4d\ ^1D$  state to the  $3pnd\ ^1F$  states in the dipole-velocity approximation. (a) represents the calculation with  $3s4f$  configuration included in the *second* term of Eq. (2) and (b) represents the calculation with  $3s4f$  configuration included in the *first* term of Eq. (2).

TABLE II. The calculated excitation energies  $E_{\text{exc}}$  (from the  $3s3d\ ^1D$  state) and the widths  $\Gamma$  for the doubly excited  $3pnl\ ^1F$  autoionization series. The columns  $A$  represent values calculated with  $3s4f$  configuration included in the second term  $\Phi_{\nu\mu}$  of Eq. (2) and columns  $B$  represent values with the  $3s4f$  configuration included in the first term of Eq. (2). The values given in parentheses are calculated with the multiconfiguration bound component  $\Phi_{\nu\mu}$  alone. The widths for all  $3png\ ^1F$  states are very small (not listed) with values ranging from 0.001 to 1.0  $\text{cm}^{-1}$  in different calculations.

State	$E_{\text{exc}}\ (10^4\ \text{cm}^{-1})$		$\Gamma\ (\text{cm}^{-1})$	
	$A$	$B$	$A$	$B$
$3p3d$	3.957 (3.963)	3.959 (3.924)	703 (670)	851 (938)
$3p4d$	4.450 (4.448)	4.451 (4.439)	412 (392)	483 (478)
$3p5d$	4.680 (4.679)	4.680 (4.675)	245 (227)	287 (269)
$3p6d$	4.806 (4.806)	4.806 (4.804)	153 (141)	180 (164)
$3p7d$	4.883 (4.883)	4.883 (4.882)	101 (92)	120 (107)
$3p5g$	4.666 (4.666)	4.666 (4.665)		
$3p6g$	4.799 (4.798)	4.799 (4.798)		
$3p7g$	4.879 (4.879)	4.879 (4.878)		

would seem that the short-range interaction described above would be represented correctly by including the  $3s4f$  configuration as a part of the bound components in the second term of the state wave-function expansion given in Eq. (2). However, the close qualitative agreement between the two calculations  $A$  and  $B$  employed in the present study would make it difficult to determine which of these two treatments is the more appropriate one. Therefore, an experimental measurement for transitions from the excited states would not only lead to a more comprehensive understanding of the multielectron

interaction in the transitions dominated by the doubly excited autoionization states for the alkaline-earth atoms but also provide the necessary experimental confirmation in the establishment of a realistic theoretical treatment.

#### ACKNOWLEDGMENT

This work is supported by the National Science Foundation under Grant Nos. PHY-84-08333 and PHY-86-09966.

<sup>1</sup>D. Rassi, V. Pejcev, T. W. Ottley, and K. J. Ross, *J. Phys. B* **10**, 2913 (1977); S. Trajmar, in *Electronic and Atomic Collisions*, edited by G. Watel (North-Holland, New York, 1978), p. 113.

<sup>2</sup>J. P. Resss, C. E. Burkhardt, W. P. Carter, and J. J. Leventhal, *Phys. Rev. A* **29**, 985 (1984); W. Fiedler, Ch. Kortenkamp, and P. Zimmermann, *ibid.* **36**, 384 (1987).

<sup>3</sup>G. Mehlman-Balloffet and J. M. Esteva, *Astrophys. J.* **157**, 945 (1969).

<sup>4</sup>W. H. Parkinson, E. M. Reeves, and F. S. Tomkins, *J. Phys. B* **9**, 158 (1976); R. H. Hudson, V. L. Carter, and P. A. Young, *Phys. Rev.* **180**, 77 (1969).

<sup>5</sup>G. H. Newson, *Proc. Phys. Soc. London* **87**, 975 (1966).

<sup>6</sup>U. Fano, *Phys. Rev.* **124**, 1866 (1961).

<sup>7</sup>D. J. Bradley, C. H. Dugan, P. Ewart, and A. F. Purdie, *Phys. Rev. A* **13**, 1416 (1976); D. J. Bradley, P. Ewart, J. V. Nicholas, J. R. D. Shaw, and D. G. Thompson, *Phys. Rev. Lett.* **31**, 263 (1973).

<sup>8</sup>R. E. Bonanno, C. W. Clark, and T. B. Lucatorto, *Phys. Rev. A* **34**, 2082 (1986).

<sup>9</sup>T. N. Chang, *Phys. Rev. A* **37**, 4090 (1988).

<sup>10</sup>T. N. Chang, *Phys. Rev. A* **36**, 447 (1987).

<sup>11</sup>T. N. Chang and Y. S. Kim, *Phys. Rev. A* **34**, 2609 (1986).

<sup>12</sup>T. N. Chang, *Phys. Rev. A* **34**, 4550 (1986).

<sup>13</sup>C. Bottcher and A. Dalgarno, *Proc. R. Soc. London, Ser. A* **340**, 187 (1974).

<sup>14</sup>T. N. Chang, *Phys. Rev. A* **36**, 5468 (1987).